



## Effects of the Inhomogeneous Loading of Magnetic Nanoparticles in Thermoseeds for Bone Tumors Hyperthermia

Matteo Bruno Lodi <sup>(1)</sup>

(1) Department of Electrical and Electronic Engineering, University of Cagliari, via Marengo 2, 09123, Cagliari, Italy

### Abstract

Bone tumors can be treated by delivering local hyperthermia by exposing to a radiofrequency magnetic field implanted biomaterials loaded with magnetic nanoparticles. To date, the manufacturing of this kind magnetic thermoseeds can result in significantly inhomogeneous loading patterns, which can drastically affect the quality and outcome of the hyperthermia treatment. Beside this aspect, the problem of reliably assessing the specific absorption rate and the therapeutic potential of so-called magnetic scaffolds arise. This work deals with the investigation of the effects of inhomogeneous loading on the hyperthermia treatment of bone tumors. To this aim, numerical, multiphysics studies are carried out to elucidate if and how the magnetic nanoparticles distribution can affect the hyperthermia treatment.

### 1. Introduction

Bone tumors (BT) are neoplasms affecting hard tissues, causing pain, frequent pathologic fractures and ruining the patients' quality of life [1]. Primary or secondary BT can be radio- and chemo-resistant, with an average 5-years survival rate of about 30-40%, showing a metastatic rate of ~20%, thus demanding for tumor resection and limb sparing surgery [2]. However, some clinical limitations remains to be addressed. As first, high recurrence rate of about 40%, due to unclear margins and residual cancers cells, was reported [1]-[3], thus alternative and innovative treatment modalities must be developed. Hyperthermia treatment (HT), whose aim is to increase the temperature of a target tissue in the range 41-44°C by providing external energy (e.g., ultrasound, electromagnetic), was proposed as a new therapeutic modality [4]. HT against bone tumor can be an effective therapy, due to the boost of the immune response, the impair of DNA repair mechanisms, generation of reactive oxygen species, the alteration of tumor microenvironment, and the increase of permeability to chemotherapeutics and the augmentation of radio-sensitivity [4]. Thus, it can be a powerful alternative to the gold standard resection, but also to microwave ablation, which resulted in marginal clinical improvements and could damage the treated bone tissue, thus calling for bone grafts or implants [3].

These limitations lead to investigation and development of new engineering tools capable to allow to perform the local HT and to provide, also, the mechanical and biocompatibility features required for a proper post-operative management [5]-[7]. The loading of magnetic nanoparticles (MNPs), which can be ferro-, ferri- or superparamagnetic, in a polymeric or bioceramic biomaterial result in a so-called magnetic scaffold (MS) [5]-[7]. The MS can be implanted after the tumor resection, an external radiofrequency (RF) magnetic field (MF) can be applied to cause the heat dissipation of MNPs and perform the HT against the residual bone tumor cells, as shown in Fig. 1. In this way radio- and chemotherapy effectiveness can be enhanced and the recurrence can be controlled [1]-[4]. After the treatments, the MS could support the healthy bone tissue regeneration providing mechanical and biological support.

The success and quality of the local HT of bone tumors performed using MS depends on the extrinsic treatment parameters (i.e., strength, homogeneity and working frequency of the MF), but, mainly, on the MS magnetic properties [8]-[10]. The manufacturing approach of MS can strongly affect the magnetic features and the heat dissipation. In particular, the loaded fraction of MNPs ( $\phi_m$ ) and the saturation magnetization ( $M_s$ ) are pivotal properties [7], [10]. MS can be obtained by chemical or physical route [8], [10]. Chemical methods, such as doping with magnetic ions (e.g., Fe, Ni, Pt, etc.), are usually employed to obtain magnetic bio-ceramics and glass-ceramics [7], [10]. The physical route is typically used for loading MNPs in polymers (e.g., PLA, PCL, PMMA), such as by electrospinning, impregnation, dip-coating, blending and 3D printing [10]. However, the aforementioned manufacturing methods suffers from controllability issues. Ferrofluid impregnated MS exhibited a  $\pm 20\%$  variation of the saturation magnetization in a volume of 5 mm [8]. Therefore, recently the hypothesis that the inhomogeneous loading of MNPs in MS could affect the outcome of the HT was investigated [10]. Indeed, the non-uniform distribution of MNPs can lead to local peaks of the specific absorption rate (SAR), which can strongly impact on the temperature pattern, thus calling for a dedicated treatment planning framework. Given the aim of performing a high quality thermal therapy, a study dealing with the evaluation of the relationship between the loading patterns of MNPs and the

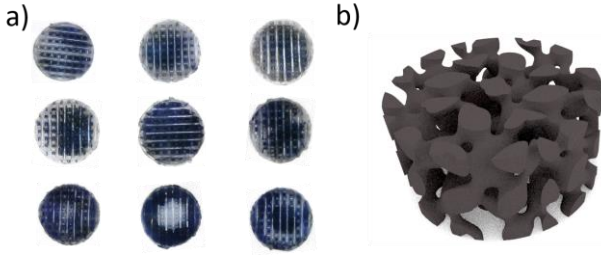


**Figure 2.** Examples of magnetic scaffolds (MS). a) MS obtained with a dip-coating procedure carried out in presence of a static magnetic field and using magnetic nanocrystals [10]. b) 3D-printed MS made of a PLA loaded with iron particles and with a complex architecture.

HT of bone tumor is mandatory. This work will address this problem by critically analyzing the literature and reviewing the characterization methods in Sect. 2. The method developed for performing numerical and multiphysics simulations for selected case studies is described in Sect. 3. Results and Conclusions are provide in Sect. 4 and 5, respectively.

## 2. Magnetic Nanoparticles Distributions

### 2.1 Experimental Evidences

The ferrofluid-impregnated MS in [8] are the first example demonstrating that manufacturing magneto-responsive biomaterial can result in strongly variable patterns. In [9], by using a nonlinear multiphysics model, a MNPs distribution decreasing from the periphery to the center of a cylindrical biomaterial was considered. With numerical experiments, it was shown that the amplitude of MF RF would significantly differ for the HT of bone tumors performed using a homogeneously or inhomogeneously loaded MS. In [10], a specific, modified dip-coating procedure was developed to obtain a desired distribution of MNPs in the biomaterial volume. In detail, under the action of an external Nd-Fe-B magnet, a ferrofluid is dripped onto polymeric scaffolds, and the distribution is controlled by creating a mask with adhesive tape. Examples of MS are shown in Fig. 2. These findings from the literature demands for a deeper understanding of the role of MNPs pattern in MS in HT of bone tumors. However, to study the problem by using rigorous theoretical electromagnetic models or numerical solutions, the MNPs distribution has to be recovered.

### 2.2 Methods for Characterization

The problem of recovering the spatial distribution of MNPs inside the biomaterial after the manufacturing procedure is an underestimated problem [5]-[10]. Therefore, there is no standardize methodology to solve this problem. Static magnetic measurements of  $M_S$  can be carried out by sampling the scaffold and extracting small sub-volumes to be used with vibrating sample magnetometry (VSM) or superconducting quantum interference devices (SQUID)

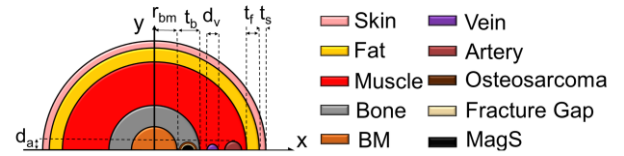


**Figure 3.** Simplified 2D axisymmetric geometry for a human upper limb affected by a bone tumor, which is surgically reduced, and treated with an implanted MS, having a inhomogeneous MNPs distribution.

[8]. However, this approach is a time-demanding and costly solution, which cannot cover the entire biomaterial volume. Scanning electron microscopy, working in energy dispersive X-ray spectroscopy, is a destructive technique which allows to map the elemental distribution but in small region of the sample [10]. Magnetic resonance imaging (MRI) could be used to derive the distribution of the transverse relaxation time  $T_2$  in the scaffold, despite being a tomographic approach, this is a costly equipment and the spatial resolution is limited. The use of magnetic particle imaging (MPI) as investigation and characterization technique ensure a resolution of  $\sim 0.5-1$  mm [11], which may not be enough for magnetic bone implants of small size ( $\sim 5$  mm). Recently, THz time-of-flight imaging (40 GHz-3 THz) was proposed as a nondestructive characterization technique for MS [10]. Despite demanding ad hoc processing procedures, in [10] it was demonstrated that the thickness of the sample, the refractivity index and the MNPs distribution map can be derived and used in numerical simulations by fitting it using a finite series of radial basis functions.

## 3. Multiphysics Numerical Modeling of Bone Tumor Hyperthermia with Magnetic Scaffolds

Having reported the experimental facts showing that MNPs distribution in MS must be considered as inhomogeneous, HT of bone tumors with these multifunctional and magneto-responsive biomaterials must be planned in silico to investigate properly the relevant parameters and study the impact on the SAR and temperature patterns.

We study the HT of bone tumors for the case of a surgically removed tumor in the human upper limbs [9]. The geometry is shown in Fig. 3.

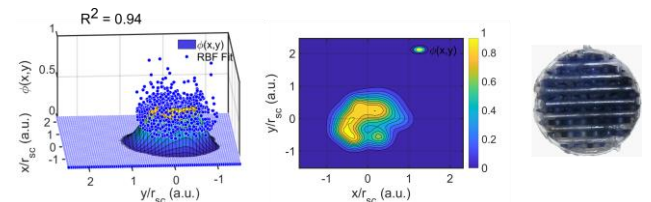


**Figure 4.** Example of the fitting of MNPs distribution in MS inputed to the multiphysics numerical model of bone tumor HT.

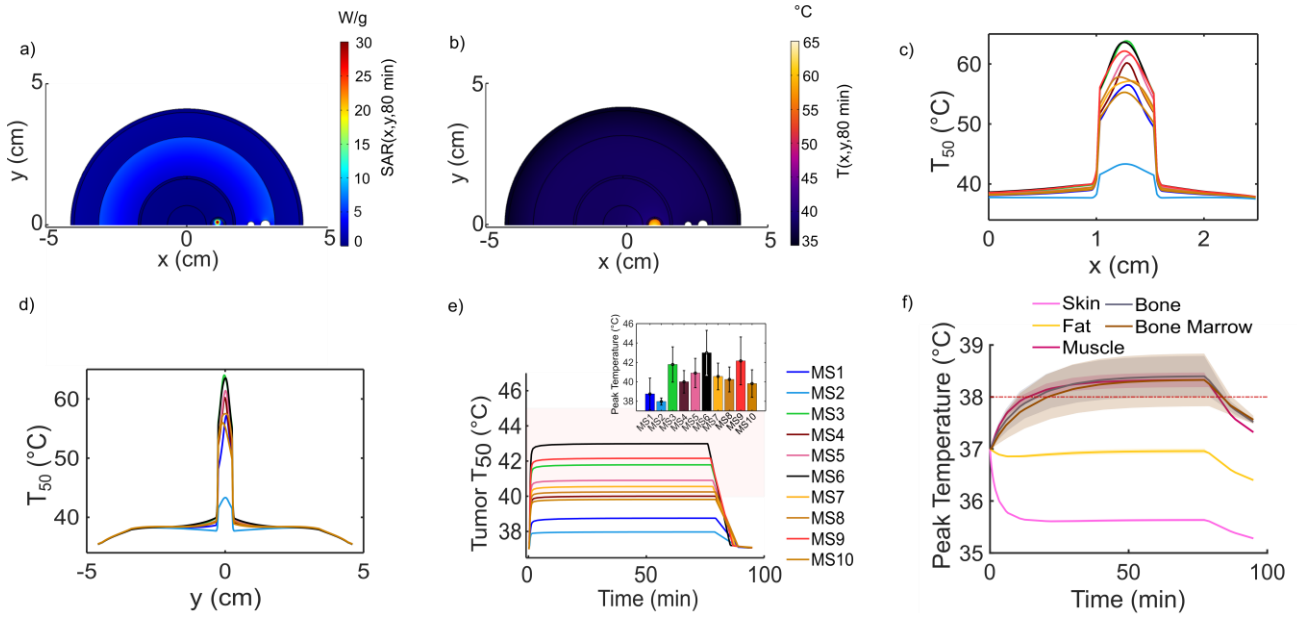


**Figure 5.** a) SAR (in  $\text{Wg}^{-1}$ ) distribution in the MS and biological tissues. b) Temperature pattern (in  $^{\circ}\text{C}$ ) at  $t = 80$  min. c)  $T_{50}(x, 0, t)$  for all MS. d)  $T_{50}(0, y, t)$  for all MS. e)  $T_{50}(t)$  in the region of residual cancer cells vs. time. f) Maximum temperature in non-target tissues, averaged over all tested MS.

The HT is assumed to be carried out by applying an external RF MF, whose source is a solenoid coil with 50 turns, a length of 28.5 cm and a diameter of 10.5 cm [9], [10]. The field is turned on after 1 min and off after 80 min. With this background field, the Maxwell's equation are solved in the frequency domain using the finite element commercial software Comsol Multiphysics (Comsol Inc., Burlington MA USA). The complex magnetic susceptibility,  $\chi$ , is assumed to be i) a function of frequency ( $f$ ), modeled with a Cole-Cole law [9]; ii) a non-linear function of system temperature [9], and iii) a function of  $xy$ -coordinates, so that  $\chi = \chi(f, T, x, y)$ . The properties of MS are taken from [10]. The dielectric properties of tissues are assumed to vary linearly with temperature as in [9]. The distribution of MNPs,  $\phi(x, y)$ , in the scaffold region (Fig. 3) was derived from the data from [10] for the case of ten MS, defined therein as  $\text{MS}_i$ , with  $i = 1, \dots, 10$ . In detail, the distribution from the time-of-flight THz image is fitted to a finite series of radial basis function (RBF), i.e.

$$\phi(x, y) = \sum_{q=1}^{N=8} a_q e^{-b_q \left[ \sqrt{(x-x_{0,q})^2 + (y-y_{0,q})^2} \right]^2} \quad (1)$$

The total, space-varying electromagnetic power ( $Q_{EM}$ ) is computed, the SAR is derived and used to solve, by using the Bio-Heat Transfer module, the non-linear Pennes' equation, considering the temperature-variation of the thermal conductivity, heat capacity and blood perfusion of tissues [9], to compute the spatio-temporal distribution of temperature  $T$ . As figure of merit for assessing the treatment quality the  $T_{50}$  is considered.

## 4. Results

By using approximated MNPs distribution  $\phi(x, y)$  derived from [10] (Fig. 4), the coupled electromagneto-thermal model ruling the HT of bone tumors with MS was solved. The pattern of MNPs in the biomaterial leads to an inhomogeneous distribution of SAR, as can be observed in Fig. 5.a. For the treatment quality, this implies that additional attention must be paid, in advance, during the crucial treatment planning phase, in order to avoid excessive overheating and local spot in non-target tissues. As regards bio-nanomaterial science, this finding allows to forecast the development of optimized and controllable manufacturing approaches. However, in the field of hyperthermia, given the result from Fig. 5.a, a concern about the methodology for quantifying and measuring the SAR rise. Therefore, suitable, reliable and valid protocols has to be developed.

From the SAR distribution, the temperature pattern can be estimate, as shown in Fig. 5.b. Noticeable temperature gradients can be noticed in the MS, as can be seen along the two main axis in Figs. 5.c and 5.d, thus implying that the heat transfer phenomena from the thermoseed to the target tumor region is far more complex than that previously assumed [9]. Considering a set of MS (see Fig. 2), and testing them, the  $T_{50}$  in the tumor result to be difficult to control, at fixed MF amplitude and  $f$ , as shown in Fig. 5.e. This is due to several factors, such as the difficulty in controlling the average MNPs content and due to the fact that the MNPs pattern result in a non-homogeneous temperature distribution (inset in Fig. 5.e). As regards the non-target tissues, in particular the healthy bone and bone marrow, the maximum average temperature over time is shown in Fig. 5.f. Temperature increases of maximum  $1.5^{\circ}\text{C}$  can be achieved. Therefore, if the MNPs

pattern can be shaped and controlled, also the requirement of non-target tissues safety could be satisfied.

## 5. Conclusions

This work dealt with the investigation of the influence of inhomogeneous loading patterns of magnetic nanoparticles in biomaterials implant meant to be used as thermosteds to perform local hyperthermia treatment of bone tumors. The issues and limitations of current manufacturing methods of magnetic scaffolds are analyzed. Possible characterization methods to derive the MNPs pattern are reviewed. With this knowledge, numerical simulations with a nonlinear multiphysics model are carried out. The analysis of SAR and of temperature dynamics and patterns highlight that robust and controllable manufacturing methods must be developed, while showing that further development in the treatment planning is required, but also indicating that reliable methods for estimating the SAR and therapeutic potential are needed.

## 6. Acknowledgements

This work is relevant to the aims and objectives of WG2 from COST Action 17115 MyWave.

## References

- [1] A. Luetke, et al., "Osteosarcoma treatment—where do we stand? A state of the art review," *Cancer Treatment Reviews*, **40**, 4, pp. 523-532, 2014. doi: 10.1016/j.ctrv.2013.11.006.
- [2] C. Meazza, S. Bastoni, P. Scanagatta, "What is the best clinical approach to recurrent/refractory osteosarcoma?," *Expert Review of Anticancer Therapy*, **20**, 5, pp. 415-428, 2020. doi: 10.1080/14737140.2020.1760848.
- [3] K. Han, et al., "Is limb salvage with microwave-induced hyperthermia better than amputation for osteosarcoma of the distal tibia?," *Clinical Orthopaedics and Related Research*<sup>®</sup>, **475**, 6, pp. 1668-1677, 2017. doi: 10.1007/s11999-017-5273-1.
- [4] N. R. Datta, S. Gomez Ordonez, U. S. Gaipal, M. M. Paulides, Hans Crezee, J. Gellermann, D. Marder, E. Puric, S. Bodis, "Local hyperthermia combined with radiotherapy and/or chemotherapy: Recent advances and promises for the future," *Cancer Treatment Reviews*, **41**, 9, pp. 742-753, 2015. doi: 10.1016/j.ctrv.2015.05.009.
- [5] A. Baeza, D. Arcos, M. Vallet-Regi, "Thermosteds for interstitial magnetic hyperthermia: from bioceramics to nanoparticles," *Journal of Physics: Condensed Matter*, **25**, 48, p. 484003, 2013. doi: 10.1088/0953-8984/25/48/484003.
- [6] M. Banobre-Lopez, Y. Pineiro-Redondo, M. Sandri, A. Tampieri, R. De Santis, V. A. Dediu, J. Rivas, "Hyperthermia induced in magnetic scaffolds for bone tissue engineering," *IEEE Transaction on Magnetism*, **50**, 11, pp. 1-7, 2014. doi: 10.1109/TMAG.2014.2327245.
- [7] M. Miola, Y. Pakzad, S. Banijamali, S. Kargozar, C. Vitale-Brovarone, A. Yazdanpanah, O. Bretcanu, A. Ramedani, E. Verne, and M. Mozafari, "Glass-ceramics for cancer treatment: so close, or yet so far?" *Acta Biomaterialia*, **83**, pp. 55-70, 2019. doi: 10.1016/j.actbio.2018.11.013.
- [8] A. Riminucci, C. Dionigi, C. Pernechele, G. De Pasquale, T. De Caro, G. M. Ingo, F. Mezzadri, N. Bock, M. Solzi, G. Padeletti, M. Sandri, A. Tampieri, V. Dediu, "Magnetic and morphological properties of ferrofluid-impregnated hydroxyapatite/collagen scaffolds," *Science of Advanced Materials*, **6**, 12, pp. 2679-2687, 2014. doi: 10.1166/sam.2014.1986.
- [9] M. B. Lodi, A. Fanti, G. Muntoni, G. Mazzarella, "A Multiphysic Model for the Hyperthermia Treatment of Residual Osteosarcoma Cells in Upper Limbs Using Magnetic Scaffolds," *IEEE Journal on Multiscale and Multiphysics Computational Techniques*, **4**, pp. 337-347, 2019. doi: 10.1109/JMMCT.2019.2959585.
- [10] M. B. Lodi, et al., "Influence of Magnetic Scaffold Loading Patterns on their Hyperthermic Potential against Bone Tumors," *IEEE Transactions on Biomedical Engineering*, 2021. doi: 10.1109/TBME.2021.3134208.
- [11] J. Rahmer, et al., "Analysis of a 3-D system function measured for magnetic particle imaging," *IEEE Transactions on Medical Imaging*, **31**, 6, pp. 1289-1299, 2012. doi: 10.1109/TMI.2012.2188639.